Science of the Total Environment 792 (2021) 148321

Contents lists available at ScienceDirect

Science of the Total Environment

journal homepage: www.elsevier.com/locate/scitotenv

Spatiotemporal effects of interacting water quality constituents on mercury in a common prey fish in a large, perturbed, subtropical wetland☆

Peter Kalla [a,*], Michael Cyterski [b], Daniel Scheidt [c], Jeffrey Minucci [d]

[a] United States Environmental Protection Agency, Region 4, Laboratory Services and Applied Science Division, 980 College Station Road, Athens, GA 30605, USA
[b] United States Environmental Protection Agency, Office of Research and Development, Center for Environmental Measurement and Modeling, Environmental Processes Division, 960 College Station Road, Athens, GA 30605, USA
[c] United States Environmental Protection Agency, Region 4, Water Division, 980 College Station Road, Athens, GA 30605, USA
[d] United States Environmental Protection Agency, Office of Research and Development, Center for Public Health and Environmental Assessment, Public Health and Environmental Systems Division, Research Triangle Park, 109 TW Alexander Drive, Durham, NC 27709, USA

HIGHLIGHTS

- We characterized 45 environmental variables in the Everglades over 20 years.
- We measured those variables in biota, water, detrital matter, and soil.
- Generalized Boosted Models identified important covariates of Hg in a prey fish.
- Sulfur, phosphorus, and organic carbon can interact to influence Hg biomagnification.

GRAPHICAL ABSTRACT

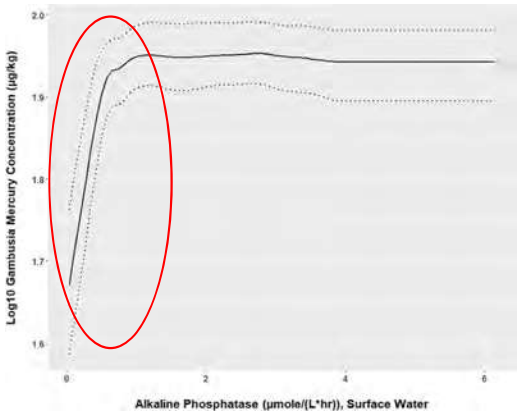

ARTICLE INFO

Article history:
Received 26 January 2021
Received in revised form 3 June 2021
Accepted 4 June 2021
Available online 9 June 2021

Editor: Xinbin Feng

Keywords:
Everglades
Mosquitofish
Phosphorus
Sulfur

ABSTRACT

We present results of a multiyear study of the Everglades (Florida, USA) detailing how differences in environmental variables can alter mercury concentrations in the food web. About 1000 random locations throughout the freshwater Everglades marsh have been sampled for the United States Environmental Protection Agency's Everglades Regional Environmental Monitoring and Assessment Program ("REMAP") since 1995. REMAP sampling is synoptic and multimedia, including an abundant prey fish (eastern mosquitofish, *Gambusia holbrooki*) as an indicator of mercury bioaccumulation. Amplifying an approach we reported to Everglades National Park, we used Generalized Boosted Models on the REMAP data to estimate how much of the mercury concentration in mosquitofish could be explained by water quality constituents or indicators of ecological health (covariates). The resulting model accounts for 60% of the environmental influence on variation in mosquitofish mercury, a robust outcome for a large, disturbed ecosystem such as the Everglades, given its seasonal, annual, and spatial differences. Of the eight most influential covariates, two were methyl mercury in periphyton and water, two can be indicators of trophic state (alkaline phosphatase and chlorophyll-*a*), one can be a marker of stormwater transport (conductivity), and two can be enablers of mercury methylation (sulfate in soil and water). While these covariates had an average individual influence ranging from 4.0% to 10.1%, together they accounted for 52.2% of the

☆ The views expressed in this article are those of the authors and do not necessarily represent the views or policies of the U.S. Environmental Protection Agency.

* Corresponding author.
E-mail address: kalla.peter@epa.gov (P. Kalla).

https://doi.org/10.1016/j.scitotenv.2021.148321
0048-9697/

Habitat
Restoration

total relative influence. Water with low phosphorus, but with sulfur and carbon above background, moved into the less disturbed parts of the Everglades via modifications to the existing water management system, could increase mercury bioaccumulation in those parts of the marsh.

1. Introduction

Mercury contamination of fish, including gamefish, and wildlife in the Florida Everglades (USA) has been a concern of agencies that manage natural resources and a focus of research and monitoring since the 1990s (Scheidt and Kalla, 2007). Fish consumption advisories are in place for several species of gamefish throughout the Everglades (FDOH, 2019). Ecological risk assessments and mercury dosing studies have indicated that populations of top predators in the Everglades could be adversely affected by mercury contamination, in that mercury accumulation through the food web has the potential to reduce the health or breeding success of wading birds (Spalding et al., 2000; Duvall and Barron, 2000; Rumbold, 2005, 2019b; Rumbold et al., 2008; Zabala et al., 2020) and the Florida panther (Barron et al., 2004; Rumbold, 2019b).

Inorganic mercury deposited into surface water from the atmosphere can be converted to methylmercury (MeHg) by bacteria in the presence of sulfate (Orem et al., 2011) and organic carbon (Aiken et al., 2011). Sulfate-reducing anaerobic bacteria have most often been associated with robust mercury methylation in the literature, though many other anaerobes, notably iron reducers and methanogens, have also been reported as methylators (Regnell and Watras, 2019). Methylmercury is the toxic form of mercury that strongly bioaccumulates and biomagnifies in the aquatic food chain (Hammerschmidt and Fitzgerald, 2006; Seixas et al., 2014). Atmospheric deposition is the predominant source of mercury to the Everglades (FDEP, 2013). It is estimated that 85% to 95% of the mercury deposited on the Everglades comes from sources outside of the United States (reviewed in Vijayaraghavan and Pollman, 2019).

Data on mercury contamination from Everglades REMAP have been modeled by previous investigators, notably Thornton (in Stober et al., 2001) and Pollman (2014). These efforts were undertaken approximately midway through the history of REMAP. They featured structural equation modeling, and included variables that implicitly reflect trophic state and habitat quality. The present study is based on a different modeling technique applied to all REMAP data to date (USEPA, 2021), and it builds on their work to explore further the relationships between mercury methylation, trophic state, and habitat quality, and resultant efficiency of mercury biomagnification. This paper is an outgrowth of earlier work done for Everglades National Park (Kalla et al., 2019), using a similar model structure but with a modified approach to handling the data and generating model outputs. In the earlier work we parsed the data by year and season of collection, and we included no results on the variability of the model outputs. Here, we refine our analysis by focusing on a single model that spans all years and seasons, after removing those covariates found to be highly correlated with other covariates, to facilitate a clearer interpretation of covariate importance in the final model. We also include confidence intervals and standard deviations for the relationships.

The objective of our work was to characterize relationships between measured covariates and mosquitofish mercury levels, using a general statistical modeling framework that could enable prediction of variations in mosquitofish mercury (fish Hg) concentrations across the Everglades. This model would help identify factors that are most influential on temporal and spatial fluctuations in fish Hg. The dataset was comprised of measurements of mercury in mosquitofish and other ecosystem compartments; physico-chemical measurements of ambient waters, flocculant detrital matter (floc), and soil; and categorical environmental factors such as habitat type and geographical subarea.

2. Study area

The Florida Everglades is one of the largest freshwater marshes in the world (Ramsar Convention, 2006). In its undisturbed reaches, it is an oligotrophic wetland that is a mosaic of sawgrass, wet prairies, and sloughs, featuring calcareous periphyton as the characteristic algal community, and tree islands, some of which support subtropical species (Lodge, 2019). Periphyton is the dominant primary producer in the native marsh (Browder et al., 1994; Gaiser, 2009) and an important food source for primary and secondary aquatic consumers in the Everglades (Liston and Trexler, 2005) and elsewhere (Hart and Lovvorn, 2003). The natural periphyton community is highly sensitive to elevated phosphorus levels. Background surface water phosphorus can be as low as the laboratory analytical method detection limit of 2 μg/L (Julian, 2016). As phosphorus concentration increases above 10 μg/L, the cyanobacterial-diatom assemblage characteristic of oligotrophic conditions is replaced by filamentous green algae (McCormick and O'Dell, 1996), and the native periphyton community is lost (McCormick et al., 2009). Phosphorus-induced changes to the Everglades are systemic (Gaiser et al., 2005).

Half of this ecosystem has been lost or altered due to drainage, and concomitant urbanization to the east and conversion to agriculture to the north (Scheidt and Kalla, 2007; Rumbold, 2019a). It is also compartmentalized by two major east-west highways, one of which forms the northern border of Everglades National Park. Most of the remaining 2000 mile^2 (5180 km^2) of the Everglades is in various forms of public ownership (Davis and Ogden, 1994). To protect the Everglades from phosphorus pollution transported by canals from the Everglades Agricultural Area (EAA) up-gradient, Stormwater Treatment Areas (STAs) were constructed to intercept and treat agricultural drainage water before it reaches the marsh (Scheidt and Kalla, 2007; Kalla and Scheidt, 2017). The STAs remove little sulfate [South Florida Water Management District (SFWMD), 2016] or organic carbon (Gu et al., 2006). The Central Everglades Planning Project has been proposed to move more water from the STAs into the central Everglades for purposes of hydrological restoration (U.S. Army Corps of Engineers and SFWMD, 2014). In a separate project recently completed, flows were restored into the northeastern corner of Everglades National Park, an area where some phosphorus enrichment has been documented near inflow structures that deliver canal water. Restoration efforts must continue to avoid P-enrichment as well as identify how hydrologic restoration may interact with sources of legacy P (Sarker et al., 2020). Canals that can transport phosphorus are known to transport sulfate and organic carbon (Scheidt et al., 2000).

3. Methods

3.1. Everglades REMAP

The United States Environmental Protection Agency (USEPA) has been conducting probabilistic surveys of the Everglades marsh since the mid-1990s, an effort known as the Everglades Regional Environmental Monitoring and Assessment Program ("REMAP") (Stober et al., 2001; Kalla and Scheidt, 2017). This statistical approach to estimating ecological condition was initiated throughout the United States in the early 1990s by USEPA (Thornton et al., 1994; USEPA, 1995; Diaz-Ramos et al., 1996; Stevens Jr., 1997; Olsen et al., 1999; Stevens Jr. and Olsen, 2004), and continues to this day in the National Aquatic Resource Surveys (e.g., Olsen et al., 2019). In 10 Everglades REMAP campaigns over four phases

spanning 1995 to 2014, 1006 stratified random marsh sites have been sampled (Fig. 1).

Eastern mosquitofish (*Gambusia holbrooki*) have been sampled as part of REMAP since the 1990s because they are an ideal indicator of mercury contamination for the following reasons: They are the most abundant fish in the Everglades and are found throughout the ecosystem in all freshwater habitats; they are easily sampled by dip-netting; they are a prey fish in the food web for gamefish and wading birds, so they provide insights for both human health and ecological health; and because of their lifespan of only several months and a small home range, they integrate mercury exposure over a short time frame in a discrete area. During the five REMAP wet season sampling events, mosquitofish were collected at 94% of the 532 Everglades marsh sites, including wet prairie, sawgrass and cattail habitats. Everglades mosquitofish are a secondary consumer and have been reported to be at trophic level 2.0 to 3.0 (Loftus et al., 1998) and 4.0 to 4.5 (Williams and Trexler, 2006). They consume animal prey (crustaceans, insects, arachnids), algae, detritus and plant matter (Loftus et al., 1998).

3.2. GBM modeling

The response variable of interest was Log10 concentrations of total Hg (μg kg^{-1}) in mosquitofish from random locations in the Florida Everglades. These data ($n = 774$ stations where fish were present) were collected in the dry and wet seasons in three different time periods: the mid- to late 1990s (1995, 1996 and 1999), 2005, and 2014 (no dry season survey that year). Our analytical approach was to use Generalized Boosted Models (GBM), a non-linear decision-tree-based machine learning technique (Friedman, 2001), to determine which independent covariates in the collected data were most influential in determining fish mercury levels. The 45 covariates listed in Table 1 were collected, but not all of them were measured during all time periods or during dry season surveys, and they varied in their % of missing values, as shown in Table 1. The five covariates shown in bold had Pearson correlations >0.75 with other variables in the dataset, and the other variables had fewer missing values, so the former five were dropped to allow for more definitive interpretation of GBM results. Covariates that showed a range greater than 100 units were log10 transformed. Of these covariates with large ranges, if some of the original values were between 0 and 1, then a Log10(X + 1) transform was used, where X is the original value. Finally, a special transform was used for the two redox potentials, as they varied between large negative and large positive values:

$$Log10(ABS(X)) * Sign(X)$$

This transformation reduces the scale of the original variable, as a log transform should do, but preserves the exact original ordering of the untransformed values. It takes a variable that ranges from -1000 to 1000, for example, and creates a variable that ranges from -3 to 3.

The GBM technique addresses missing values in the covariates by designating a third branch at each decision point to represent the mean response for all observations with a missing value for the parameter in question (Greenwell et al., 2019). For example, if water temperature were the parameter under scrutiny at a certain decision point in a decision tree, then there may be one branch for observations with water temperature ≥ 15 °C, one branch for observations with water temperature < 15 °C, and a third branch for observations with a missing value of water temperature. In this manner, the model can account for potential correlations between absent data and the response variable (García-Laencina et al., 2010).

Habitat was coded as a nominal categorical factor. There were five different habitat types where the samples were collected: sawgrass marsh ($n = 430$), wet prairie ($n = 279$), cattail marsh ($n = 36$), slough ($n = 23$), and "other" ($n = 1$ pond, 4 willow, and 1 brush). Season was coded as a binary categorical factor, wet or dry. Subarea was coded as a nominal categorical factor for five different compartments within the Everglades study area: Arthur R. Marshall Loxahatchee National Wildlife Refuge, Water Conservation Area 2, Water Conservation Area 3 north of Interstate Highway 75, Water Conservation Area 3 south of Interstate Highway 75, and Everglades National Park (Fig. 1). Year was coded as a nominal categorical factor, using the five different collection years: 1995, 1996, 1999, 2005, and 2014.

Using the GBM package (version 2.1.5, Greenwell et al., 2019) in R (R Core Team, 2018), we developed a single model for the entire dataset, but we recognize that there may be potential differences in the influence of covariates over time and season. Rainfall, discharge, and water level have varied widely during REMAP due to seasonal variation from dry season to wet season, and to interannual variability. More stormwater runoff enters the Everglades from the agricultural area to the north during the summer wet season (Scheidt and Kalla, 2007). The non-linear nature of the GBM technique can capture interactive effects amongst the covariates if the tree depth is set sufficiently high.

Due to the inherent stochasticity in the results of fitting a GBM model to a given dataset (i.e., slightly different models will be produced when fitting the same dataset), we developed bootstrapped estimates of model metrics by fitting 200 GBM models to the dataset. In each bootstrap iteration, 80% of the dataset was randomly placed into a training set to fit the model, and the remaining 20% was put into a testing set to examine model predictive capabilities.

The GBM package in R has an array of model parameters that can affect the fitting process and efficacy of the eventual solution. Our choices of values for these parameters were as follows:

- Error Term: Gaussian
- Maximum Number of Trees: 10,000
- Shrinkage: 0.005
- Interaction Depth: 3
- Bag Fraction: 0.5
- Train Fraction: 1
- Minimum Number of Observations per Node: 5
- Cross-Validation Folds: 10

An in-depth discussion of these parameters can be found in the GBM package documentation (Greenwell et al., 2019). Recommendations within Greenwell et al. (2019) were followed for setting parameter values, with some modifications based on best professional judgement. Train Fraction was set to 1 because a true testing dataset was created at the start of each iteration for assessment of model predictive capabilities. In addition, out-of-sample error would be handled by examining cross-validation folds, as explained later. A Bag Fraction of 0.5 results in each successive tree in the iterative algorithm being fit to a random 50% of the observations in the training dataset, which mitigates overfitting of the training data. An Interaction Depth of 3 means that up to third-order interactions of model covariates can be captured by the model. We did not include interactions of an order greater than 3 to preserve model interpretability. The Minimum Number of Observations per Node value prevents the model from being unduly influenced by outliers or clusters of odd samples. A value of 5 was deemed suitable for an intermediate-sized dataset such as ours (n between 100 and 1000). Smaller values of the Shrinkage parameter can increase model accuracy, but at the cost of increased computational time and more trees in the optimal solution. Values between 0.01 and 0.001 are recommended; we used 0.005.

As more trees are added to a GBM solution, the training data error (RMSE) will continue to decline; the RMSE of out-of-sample data also initially declines as more trees are added, but then rises if too many trees are used, i.e., the model becomes overfit. There are several ways to determine the optimum number of trees in a GBM solution; we used 10-fold cross-validation to measure the point at which out-of-sample RMSE began to rise.

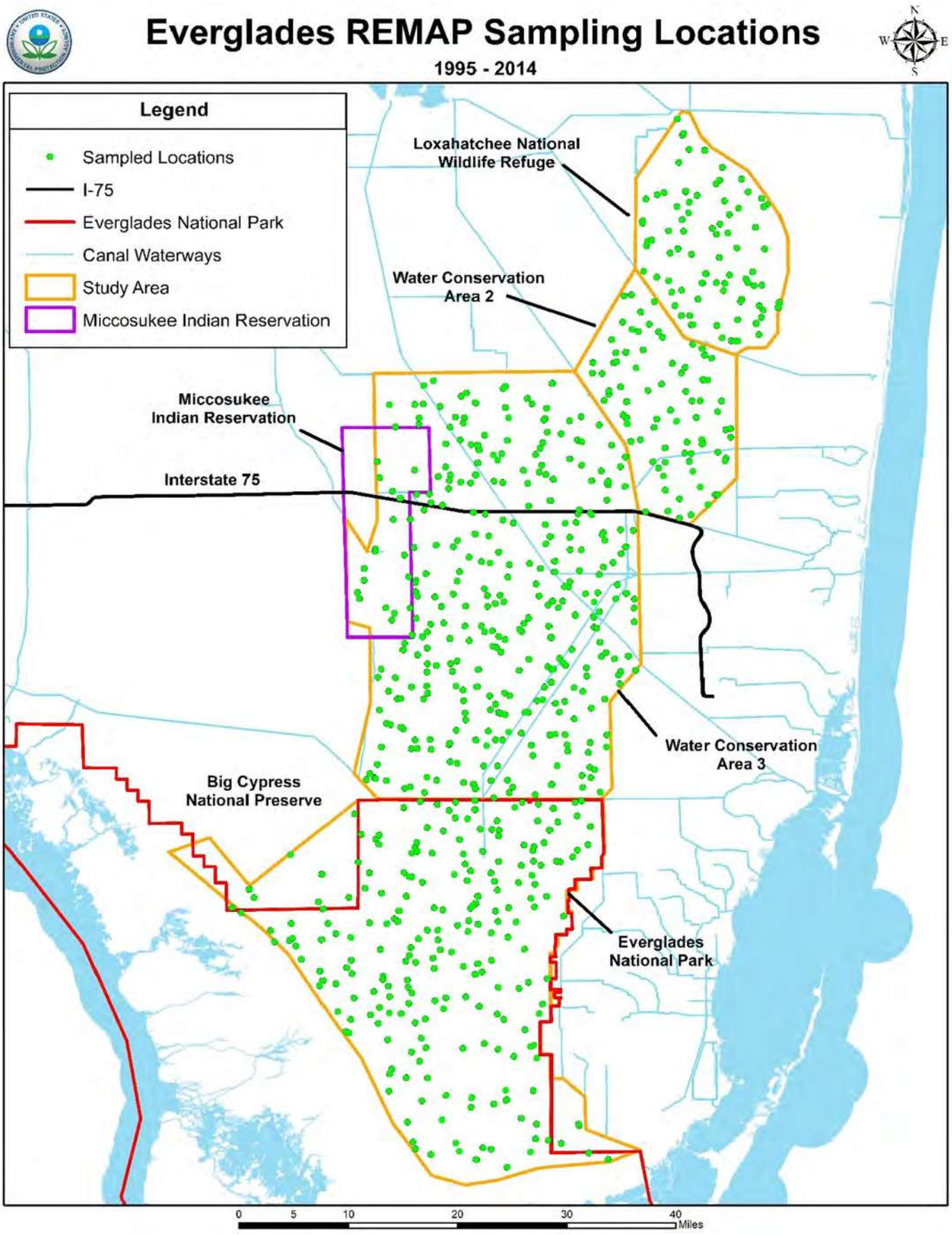

Fig. 1. Survey points for Everglades REMAP.

Table 1
Everglades REMAP covariates of total mercury in mosquitofish.

Analyte	Media	Units	% Missing	Year collected					Time periods collected
				1995	1996	1999	2005	2014	
Alkaline phosphatase activity	Surface water	µmole/L*hr	23						1995/1996/1999/2005
Ash free dry weight	**Floc**	**%**	**64**						1999/2005/2014
Ash free dry weight[1]	Soil	%	1						All
Bulk density	Floc	g/cc	64						1999/2005/2014
Bulk density	**Soil**	**g/cc**	**20**						1995/1996/2005/2014
Chlorophyll-*a*	Surface water	µg/L	65						2005/2014
Chloride	**Surface water**	**mg/L**	**46**						1999/2005/2014
Conductivity[1]	Surface water	µSiemens/cm	1						All
Depth	Floc	ft	68						1999/2005/2014
Depth	Surface water	ft	0						All
Dissolved Oxygen	Surface water	mg/L	1						All
Filtered Ammonia	Surface water	mg/L	46						1999/2005/2014
Filtered Nitrate	Surface water	mg/L	46						1999/2005/2014
Filtered Nitrite	Surface water	mg/L	46						1999/2005/2014
Habitat	–	Cattail, Sawgrass Marsh, Slough, Wet Prairie, Other	0						All
Methyl mercury	Surface water	ng/L	2						All
Methyl mercury	Floc	µg/kg	56						1999/2005/2014
Methyl mercury	Periphyton	µg/kg	40						All
Methyl mercury	Soil	µg/kg	6						All
pH	Soil	S.U.	65						2005/2014
pH	Surface water	S.U.	1						All
Redox potential[3]	Pore water	mV	16						1995/1996/1999/2005
Redox potential[3]	Surface water	mV	35						1995/1996/1999/2014
Season	–	Dry/Wet	0						All
Subarea	–	5 areas depicted in Figure 1	0						All
Soluble reactive phosphorus	Pore water	mg/L	46						1999/2005
Soluble reactive phosphorus	Surface water	mg/L	59						1999/2005/2014
Sulfate[2]	Surface water	mg/L	1						All
Sulfate[1]	Soil	µg/kg	36						1995/1996/1999
Sulfide	Pore water	mg/L	46						1999/2005/2014
Temperature	Surface water	°C	1						All
Thickness	Soil	ft	0						All
Total carbon	**Soil**	**%**	**65**						2005/2014
Total mercury	Surface water	ng/L	1						All
Total mercury[1]	Floc	µg/kg	53						1999/2005/2014
Total mercury[1]	Periphyton	µg/kg	59						1995/1996/1999/2005
Total mercury[1]	Soil	µg/kg	0						All
Total nitrogen	Surface water	mg/L	26						1996/1999/2005/2014
Total nitrogen	**Soil**	**%**	**65**						2005/2014
Total organic carbon	Surface water	mg/L	1						All
Total phosphorus[1]	Surface water	µg/L	1						All
Total phosphorus[1]	Floc	mg/kg	63						1999/2005/2014
Total phosphorus[1]	Soil	mg/kg	20						1995/1996/2005/2014
Turbidity[2]	Surface water	NTU	1						All
Year collected	–	1995/1996/1999/2005/2014	0						All

1. These covariates were Log10 transformed.
2. These covariates were $\mathrm{Log10}(X + 1)$ transformed.
3. These covariates were $\mathrm{Log10}(\mathrm{ABS}(X)) * \mathrm{Sign}(X)$ transformed.
Analytes in **bold** were dropped from the analysis. See text (Section 2, first paragraph) for explanation.

Due to the stochasticity in creating training/testing datasets, a Bag Fraction <1, and the random aliquoting of the training data into cross-validation folds, sometimes a GBM model can produce a poor solution. In each iteration of the bootstrap process, we used two metrics to ensure a GBM model was "valid":

- The optimum solution had more than 200 trees and less than 9800 trees (near to the maximum allowable, meaning convergence was achieved).
- The number of unique fitted values produced by the model was at least 25% of the total number of fitted values.

One hallmark of a poorly fit GBM model is a solution with few trees, leading to a very low number of unique fitted values. However, it is also possible to sometimes reach a good solution with a relatively small number of trees. Therefore, it is more robust to assess the quality of the model by examining the number of unique fitted values rather than the number of trees in the solution.

We ran the bootstrap algorithm until 200 valid GBM models were produced, and then computed the following characteristics for each of the seven models:

- R^2 of Actual Observations versus Model Fits for the Training Data
- R^2 of Actual Observations versus Model Fits for the Testing Data
- The Influence of the Covariates

3.3. Partial dependence plots

In order to visually inspect how each covariate influences the response variable in a model, the GBM package in R provides the ability to create Partial Dependence Plots (PDPs), which show the univariate relationship between a covariate (values plotted on the X-axis) and the response variable (values plotted on the Y-axis), while factoring out the effect of all other covariates. We created aggregate PDP plots across the 200 GBM models for covariates of interest by saving the grid of PDP points for each individual model run, and then plotting the 2.5th, 50th, and 97.5th percentiles of the y-values at each evaluated x-value.

4. Results

4.1. The GBM model

Across the 200 models, the average R^2 value for the training data was 0.90, with a standard deviation of 0.03. As expected, this was higher than the average R^2 value for the testing data, 0.58, with a standard deviation of 0.05. Fig. 2 shows a scatterplot of the average prediction for each data point versus its observed value. The average prediction for each data point is constructed using the approximately 20% of the 200 models in which the data point in question was placed into the testing data, rather than the training data. As is shown by the R^2 value in this figure, there is a slight gain incurred from making an aggregate prediction based on many GBM models versus a single GBM model (0.60 vs 0.58).

A common occurrence when using GBM to model data is a muted scale of model estimates, as seen by the slope in the regression line in Fig. 2 being <1. GBM generally does a good job of fitting the pattern of the observations, but it has difficulty with their magnitudes. The largest GBM predictions are not as large as the largest observations and are not as small as the smallest observations. The slope and intercept of the best-fit linear regression line can be used to rectify this situation by rotating the data ellipse, expanding the scale of the GBM fitted values. This rotation has absolutely no impact on the R^2 value of the model. We assume that the y-intercept of the original relationship has no interpretive meaning other than its magnitude measures the severity of this muted scale problem. The more muted the scale of the GBM estimates, the flatter the ellipse that captures the cloud of points in the scatterplot, and the larger the y-intercept.

If the regression line intercept in Fig. 2 (0.8111) is subtracted from every y-value, and then the result is divided by the slope (0.5873), an "adjusted" GBM prediction is calculated. When these adjusted values are plotted versus observations (the blue dots in Fig. 3), the R^2 value remains unchanged, but the slope and intercept become 1 and 0, as would be ideal for a plot of model predictions versus observations. The data ellipse has simply been rotated about the mean predicted GBM value. Any original GBM prediction above the mean becomes larger, while any original GBM prediction below the mean becomes smaller, i.e., the scale of the GBM predictions has been increased to match the scale of the original observations.

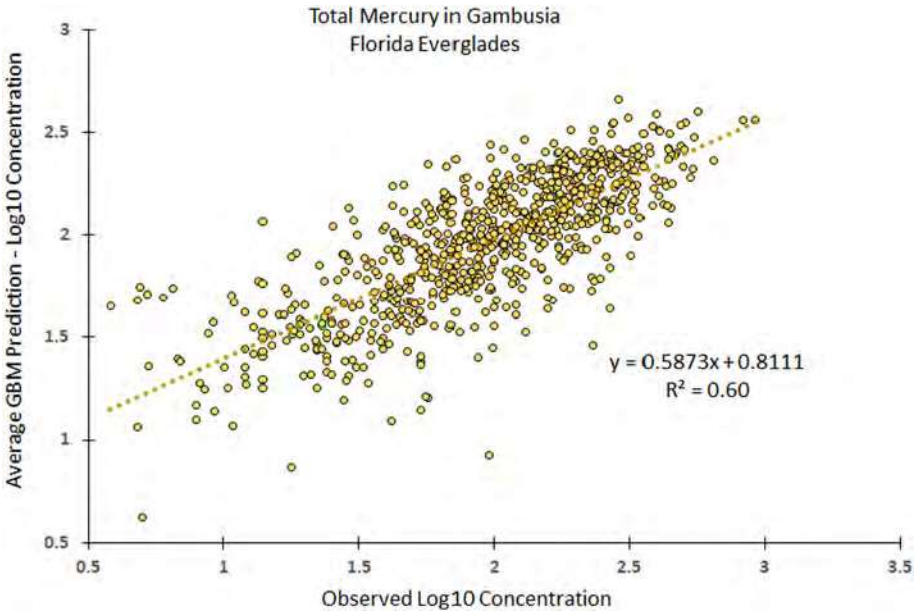

Fig. 2. Plot of GBM average predicted values (across 200 model runs) versus observations for the dataset ($n = 774$).

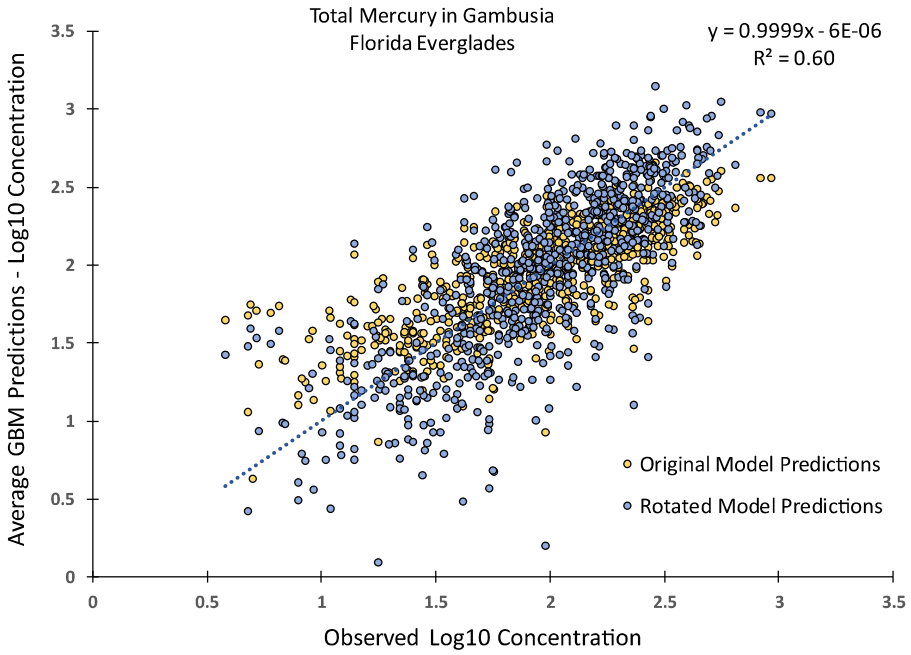

Fig. 3. Plot of the average predicted GBM values, rotated using the slope and intercept of the regression line in Fig. 2.

4.2. Influence of the covariates

Finally, we examined the influence of the covariates averaged across the 200 GBM models (Table 2). Alkaline Phosphatase Activity in surface water had the largest mean influence (10.1%), followed by Methyl Mercury in periphyton (8.0%) and Sulfate in soil (7.6%). We created PDP plots for only those covariates that accounted for at least 2% of the total influence within the dataset.

4.3. The partial dependence plots

For the PDP analysis, 17 covariates were used that had >2.0% average influence across the 200 GBM model runs. These covariates' relationships to fish Hg are plotted in Fig. 4a–h and in Fig. S1a–i in the Supplemental Information.

5. Discussion

5.1. The GBM model

The R^2 value for average predictions (Fig. 2) indicates that the GBM model accounts for 60% of the variation in mosquitofish mercury in this system. This outcome is robust for a large, disturbed ecosystem such as the Everglades, given its seasonal, annual, and spatial differences.

5.2. Sulfate and methylated mercury

The PDP for surface water sulfate (Fig. 4g) exhibits a peak in fish Hg at 2–3 mg/L sulfate, which is higher than background concentrations of <1.0 mg/L (Orem et al., 2011), down to the current USEPA method detection limit of 0.02 mg/L (Kalla and Scheidt, 2017). Other researchers found a positive correlation between net MeHg production and surface water sulfate concentrations across the Everglades over the range of 0.5–20 mg/L sulfate (Gilmour et al., 2007). Areas with intermediate concentrations of sulfate (1–20 mg/L) have sulfate and sulfide levels that promote maximum MeHg production (Orem et al., 2011). However, the PDP also shows an increase in fish Hg between 40 and 90 mg/L sulfate, which contradicts previous work that showed no increase above

Table 2
Average percent influence of examined covariates on mercury in mosquitofish across 200 GBM models; standard deviations in parentheses. PDP plots were made for the 17 covariates with ≥2% mean influence (dashed line).

Variable	Average influence (S.D.)
Alkaline phosphatase, surface water	10.1 (1.5)
Methyl mercury, periphyton	8.0 (1.1)
Sulfate, soil	7.6 (1.5)
Methyl mercury, surface water	7.3 (0.9)
Temperature, surface water	5.6 (2.9)
Conductivity, surface water	5.1 (1.0)
Sulfate, surface water	4.5 (0.7)
Chlorophyll *a*, surface water	4.0 (1.0)
pH, soil	3.2 (1.1)
Total mercury, surface water	3.2 (0.5)
Methyl mercury, soil	3.0 (0.6)
Habitat code	3.0 (0.7)
Total organic carbon, surface water	2.8 (0.5)
Total phosphorus, surface water	2.4 (0.4)
pH, surface water	2.2 (0.6)
Total phosphorus, soil	2.2 (0.4)
Dissolved oxygen, surface water	2.0 (0.7)
Redox potential, surface water	1.8 (0.3)
Turbidity, surface water	1.8 (0.5)
Water depth	1.7 (0.3)
Total nitrogen, surface water	1.6 (0.3)
Total mercury, soil	1.5 (0.4)
Redox potential, pore water	1.5 (0.3)
Ash free dry weight, soil	1.5 (0.6)
Filtered nitrite, surface water	1.5 (0.4)
Sulfide, pore water	1.4 (0.3)
Total phosphorus, floc	1.3 (0.4)
Filtered ammonia, surface water	1.3 (0.3)
Total mercury, periphyton	1.2 (0.3)
Subarea	1.1 (0.3)
Filtered nitrate, surface water	0.8 (0.2)
Soluble reactive phosphorus, surface water	0.7 (0.3)
Soil thickness	0.7 (0.2)
Methyl mercury, floc	0.6 (0.2)
Floc depth	0.6 (0.2)
Total mercury, floc	0.4 (0.1)
Bulk density, floc	0.3 (0.1)
Soluble reactive phosphorus, pore water	0.2 (0.1)
Year	0.1 (0.1)
Season	0.1 (0.1)

20–25 mg/L (Orem et al., 2011). It should be noted that the PDPs of covariates in a GBM are influenced by the other covariates in a model, as their effect is "integrated out" in order to produce the PDP for a specific covariate. In a simple GBM model with only surface water sulfate and surface water temperature as covariates of fish Hg, the PDP for surface water sulfate (Fig. 5) is closer to what would be expected based on theory, as fish mercury drops off at sulfate concentrations above 20 mg/L. Nevertheless, the full model does suggest that the influence of surface water sulfate on fish Hg extends further up the range of sulfate than what has been reported by previous investigators. Of greater significance is that fish Hg is very low at only two places on the curve, at extremely low concentrations of sulfate and at maximum sulfide inhibition of the methylation reaction (Gilmour et al., 1992) where sulfate levels are high. The upward tail in the curve at the end of the x-axis is anomalous. The wide confidence interval in that region of the curve suggests that the overall conclusion about the unimodal relationship of sulfate and fish Hg is not affected.

The PDP for sulfate in soil (Fig. 4c) has fish Hg peaking at about 500 μg kg^{-1} sulfate and then decreasing as sulfate increases, consistent with a unimodal relationship between sulfur and methyl mercury. This relationship could be explained by the activity of sulfate-reducing bacteria, which methylate mercury until inhibition by moderate to high levels of sulfide occurs (Orem et al., 2011). Since methylation in the Everglades can occur in the diurnally oxygen-depleted environment of the soil-water interface, soil sulfate can be expected to influence fish Hg.

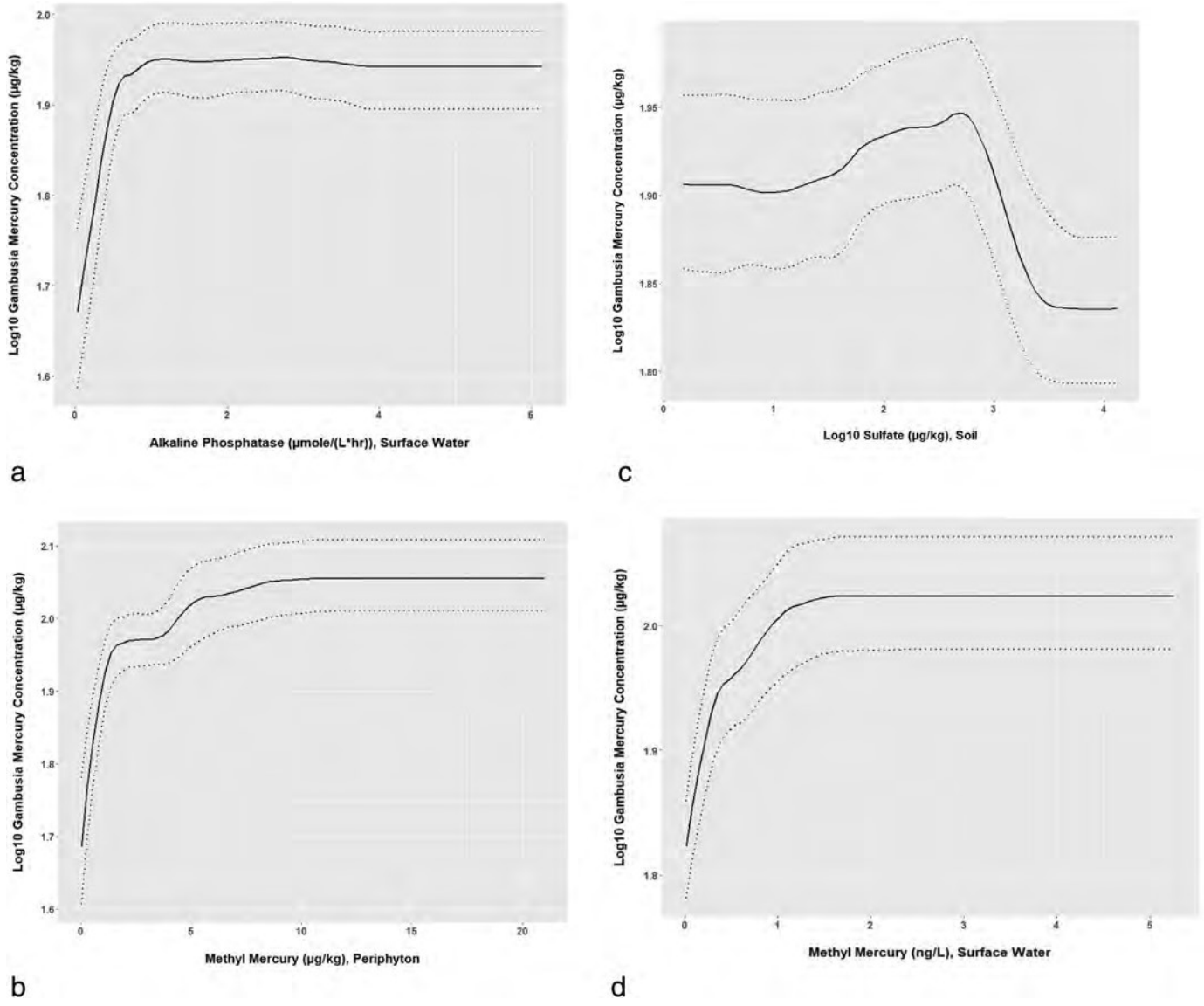

Fig. 4. a. PDP of mosquitofish Log_{10} mercury (μg kg^{-1}) on alkaline phosphatase activity (μmol L^{-1} h^{-1}) in surface water. Dashed lines represent the 2.5th and 97.5th percentiles of the variability seen in 200 GBM model runs.
b. PDP of mosquitofish Log_{10} mercury (μg kg^{-1}) on methyl mercury in periphyton (μg kg^{-1}). The dashed lines represent the 2.5th and 97.5th percentiles of the variability seen in 200 GBM model runs.
c. PDP of mosquitofish Log_{10} mercury (μg kg^{-1}) on sulfate in soil (μg kg^{-1}). The dashed lines represent the 2.5th and 97.5th percentiles of the variability seen in 200 GBM model runs.
d. PDP of mosquitofish Log_{10} mercury (μg kg^{-1}) on methyl mercury in surface water (ng/L). The dashed lines represent the 2.5th and 97.5th percentiles of the variability seen in 200 GBM model runs.
e. PDP of mosquitofish Log_{10} mercury (μg kg^{-1}) on surface water temperature (°C). The dashed lines represent the 2.5th and 97.5th percentiles of the variability seen in 200 GBM model runs.
f. PDP of mosquitofish Log_{10} mercury (μg kg^{-1}) on conductivity of surface water (μS/cm). The dashed lines represent the 2.5th and 97.5th percentiles of the variability seen in 200 GBM model runs.
g. PDP of mosquitofish Log_{10} mercury (μg kg^{-1}) on Log_{10} sulfate (mg/L) in surface water. The dashed lines represent the 2.5th and 97.5th percentiles of the variability seen in 200 GBM model runs.
h. PDP of mosquitofish Log_{10} mercury (μg kg^{-1}) on chlorophyll-*a* in surface water (μg/L). The dashed lines represent the 2.5th and 97.5th percentiles of the variability seen in 200 GBM model runs.

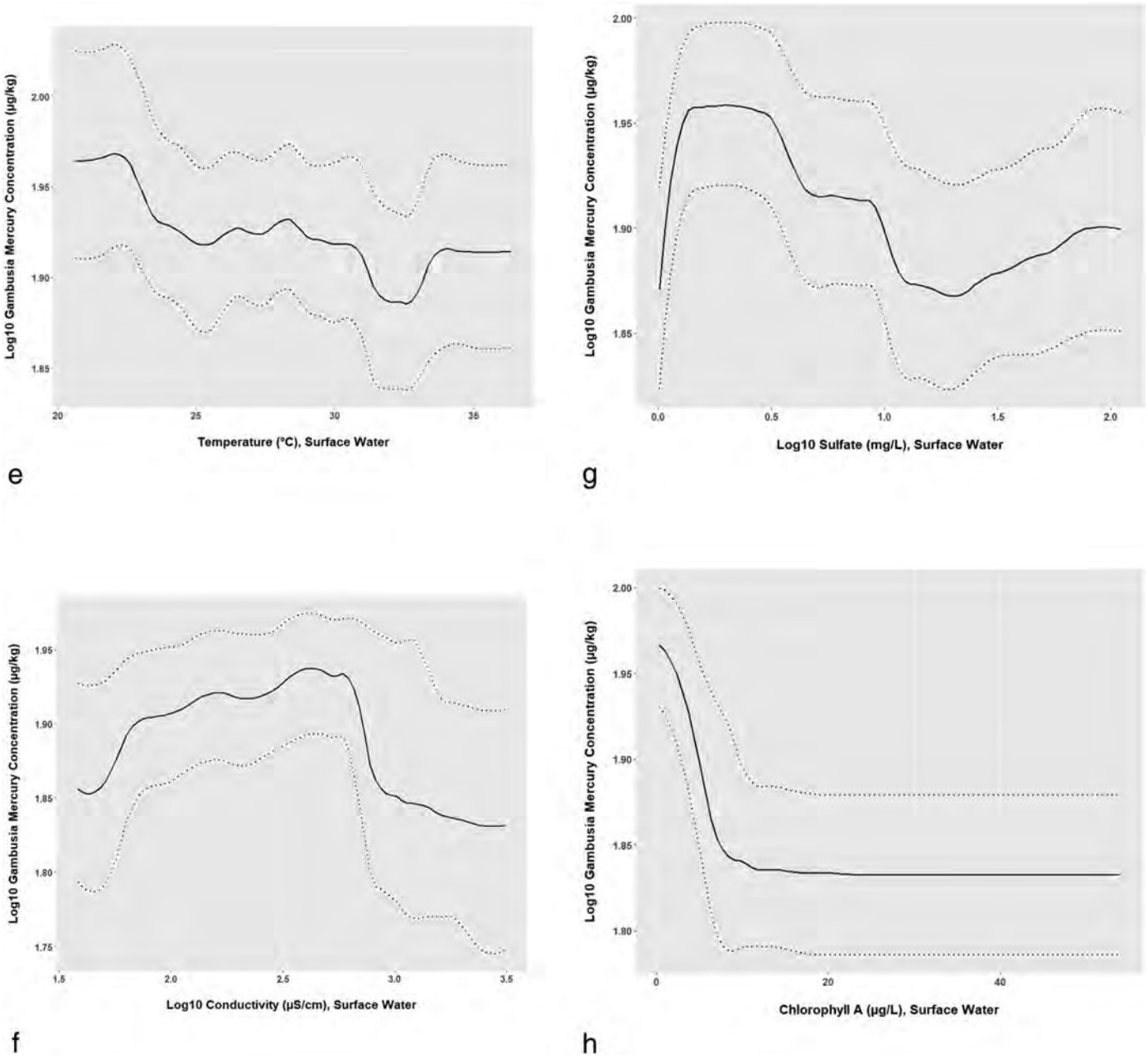

Fig. 4 (*continued*).

5.3. Other partial dependence plots

The PDPs for mercury (methyl mercury in periphyton, Fig. 4b; methyl mercury in surface water, Fig. 4d; total mercury in surface water, Fig. S1b; and methyl mercury in soil, Fig. S1c) show a largely straightforward relationship with fish Hg. Inorganic mercury enters the water from the atmosphere, is methylated, and then is taken up by biota, including periphyton, that form the food web leading to fish. The curve for methyl mercury in soil shows a slight drop after the rise probably because parts of the system with the most methyl mercury in the soil, e.g. the northern reaches of Water Conservation Area 3 (Stober et al., 2001), are where the food web has been degraded. Bioaccumulation is less in these areas (Scheidt and Kalla, 2007). The methyl mercury that cannot be efficiently incorporated into the food web is instead sequestered in the soil. Mass budget estimates based on data from the 2005 REMAP campaign showed that 58% (in the wet season) to 86% (in the dry season) of the methyl mercury produced in the ecosystem is retained in the soil, with 6% (wet season) to 9% (dry season) getting buried (Liu et al., 2008). Fluxes of mercury out of the aquatic food web have been observed in other ecosystems, e.g. Walters et al. (2020).

The curve for conductivity (Fig. 4f) resembles the curves for sulfate in Figs. 4g and 5, in that it is unimodal. All REMAP conductivity values below 100 µS/cm, toward the y-axis, were found within the Refuge, an area that has generally had lower fish Hg throughout REMAP surveys. The fish Hg peak may be spatially associated with optimal levels of other constituents needed for efficient methylation, namely those of organic carbon and sulfate (Aiken et al., 2011; Orem et al., 2011; Scheidt and Kalla, 2007). The portions of the Everglades with the highest fish Hg, WCA3 and the Park, have surface water organic carbon concentrations <20 mg/L, as reflected in Fig. S1e.

The curve for surface water pH (Fig. S1g) is, in contrast to soil pH (Fig. S1a), more straightforward. It shows a broad range of pH optimal for mercury bioaccumulation, from 6.5 to 8.0 S.U. This pH range covers

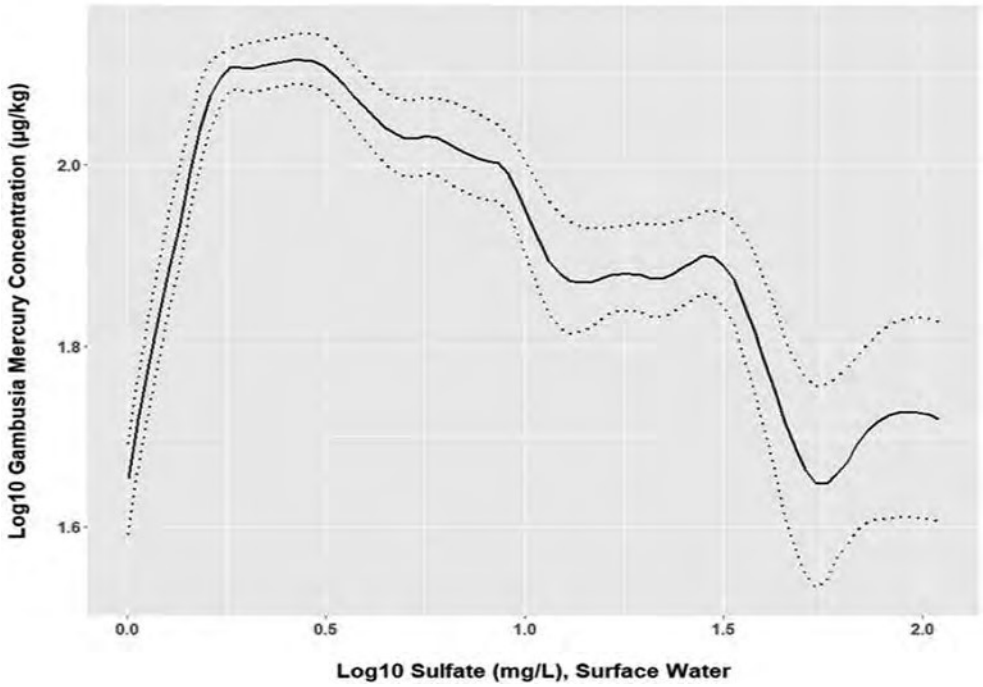

Fig. 5. PDP of mosquitofish Log_{10} mercury ($\mu g\ kg^{-1}$) on surface water sulfate (mg/L) in a model with surface water temperature as the only other covariate in the model. The dashed lines represent the 2.5th and 97.5th percentiles of the variability seen in 200 GBM model runs.

all of the Everglades except the Refuge, which has a pH of 5.5 to 7.0 (Scheidt and Kalla, 2007).

The PDP for surface water temperature (Fig. 4e), though not strictly monotonic, has the general form of lower fish Hg levels at higher temperatures. This result may be explained by sunlight. Higher temperatures tend to be found in wet prairies and sloughs during daylight because the water is less shaded than in sawgrass marshes and cattails. Photodegradation has been proposed as either the predominant mechanism of mercury demethylation in surface waters (Sellers et al., 1996; Tai et al., 2014) or a major mechanism (Sellers et al., 2001; Li et al., 2010). Fig. S1d provides corroboration for this explanation by showing that mosquitofish in wet prairies and sloughs have less mercury than those in sawgrass marshes.

There are four covariates in surface water, alkaline phosphatase activity (Fig. 4a), chlorophyll-*a* (Fig. 4h), total organic carbon (Fig. S1e), and total phosphorus (Fig. S1f), that can be associated with trophic state. Their curves show less biomagnification of mercury at higher concentrations of the covariate, except for alkaline phosphatase, which is the inverse of phosphorus because there is greater alkaline phosphatase activity in low-phosphorus environments (Newman et al., 2003). In addition to sulfur and organic carbon (Scheidt et al., 2000), agricultural runoff that enters the Everglades contains phosphorus at levels above background concentrations found in the pristine oligotrophic parts of the system, which have very low phosphorus (McCormick et al., 1999; Noe et al., 2001). Over time, this input has led to eutrophication in some areas, which in turn degraded the original habitat, producing depauperate food webs and short food chains, without calcareous periphyton at their base, which are less efficient at biomagnification (King and Richardson, 2007; Abbey-Lee et al., 2013; Pollman, 2014; Wang et al., 2014). The best example of this effect is cattail marshes, which have the least fish Hg of any habitat (Fig. S1d). Invasive cattail (*Typha domingensis*) can replace the native sawgrass (*Cladium jamaicense*) and slough communities where excessive phosphorus has accumulated in the soil (Davis, 1994; Scheidt and Kalla, 2007; McCormick et al., 2009), but even sawgrass responds to nutrient enrichment by getting taller (Stober et al., 2001). Sawgrass can be twice as tall (~2 m) and twice as dense (>50 culms/m^2) in high phosphorus locations [Richards and Kalla, unpublished results (from the 2005 REMAP campaign)]. With periphyton gone and prolonged shading by tall, dense macrophytes, the aquatic community is visibly altered. While some stable isotope work suggests that high phosphorus does not shorten food chains, it also suggests that high phosphorus changes the base of the food web from periphyton to floc derived from macrophytes (Kendall et al., 2003). Methyl mercury in floc was the seventh least influential covariate in our model, at 0.6%, whereas methyl mercury in periphyton was second most influential, at 8.0%, ranking behind only alkaline phosphatase.

The PDP for total phosphorus in soil (Fig. S1h) reflects the trophic effect as well. Fish Hg drops off starting at 100 mg/kg, well below the 500 mg/kg specified in the State of Florida's regulatory definition of Everglades locations impacted by phosphorus [Florida Administrative Code 62-302.540(3)(d)].

The curve for dissolved oxygen (DO) in surface water (Fig. S1i) rises from near 0 to about 5 mg/L and then levels off. This form also reflects trophic state, as cattail marshes, often associated with phosphorus enrichment, have the lowest DO of any habitat type in the Everglades (Belanger et al., 1989; McCormick and Laing, 2003).

5.4. Relative percent influence of covariates

Of the eight most influential covariates (those with at least 4% influence in Table 2), two were methyl mercury in periphyton and surface water, two can be trophic indicators (alkaline phosphatase and chlorophyll-*a*), one can be a marker of stormwater transport (conductivity), and two can be enablers of methylation (sulfate in soil and in surface water). While these covariates had an average individual influence ranging from 4.0% to 10.1%, together they accounted for 52.2% of the influence on fish Hg. Sulfate, the enabler, is transported to and through the Everglades by canals, along with phosphorus and organic carbon. The ecosystem receives a contaminant from the atmosphere whose presence in the aquatic food web is both mediated and mitigated by other chemical constituents in the water. As suggested by their PDPs, whereas sulfur promotes mercury methylation at optimal levels of sulfate, phosphorus acts to oppose mercury biomagnification at high levels of total phosphorus. Our model indicates that water moved into the

Everglades with low phosphorus, but sulfate and carbon above background, can influence mercury bioaccumulation in relatively pristine parts of the system where food webs are complex and based on calcareous periphyton.

Supplementary data to this article can be found online at https://doi.org/10.1016/j.scitotenv.2021.148321.

Funding

This work was supported by the USEPA ORD, South Florida Geographic Initiative, and Office of Water; Everglades National Park [Critical Ecosystem Studies Initiative grant number 5284-04-0052, and numerous Inter-Agency Agreements with EPA]; USACOE through the Monitoring and Assessment Program component of the Comprehensive Everglades Restoration Plan; FDEP; and through in-kind services provided by FWS and FDEP.

CRediT authorship contribution statement

Peter Kalla: Conceptualization, Investigation, Resources, Data curation, Writing – original draft, Writing – review & editing, Project administration, Funding acquisition. **Michael Cyterski:** Methodology, Software, Formal analysis, Writing – original draft, Writing – review & editing, Visualization. **Daniel Scheidt:** Investigation, Resources, Data curation, Writing – review & editing. **Jeffrey Minucci:** Methodology, Software, Writing – review & editing.

Declaration of competing interest

The authors declare that they have no known competing financial interests or personal relationships that could have appeared to influence the work reported in this paper.

Acknowledgements

This work was made possible by the hundreds of field samplers, sample processors, laboratory analysts, helicopter pilots, data reviewers, quality assurance officers, administrators, principal investigators, project officers, supply officers, safety officers, field electronics technicians, and spatial statisticians that participated in Everglades REMAP over the decades. These personnel came from USEPA's Region 4 and Office of Research and Development (ORD); Florida International University; the U.S. Department of the Interior's National Park Service, Fish and Wildlife Service (FWS), and Office of Aircraft Services; USEPA Region 4's in-house contractors; commercial helicopter services in Florida; the Florida Department of Environmental Protection (FDEP); the U.S. Army Corps of Engineers (USACOE); the South Florida Water Management District; Battelle Marine Sciences Laboratory; and the Miccosukee Tribe of Indians of Florida. Helpful comments on earlier drafts of this manuscript were provided by Donald Axelrad, John Davis, Curtis Pollman, Darren Rumbold, and two anonymous reviewers.

References

Abbey-Lee, R.N., Gaiser, E.E., Trexler, J.C., 2013. Relative roles of dispersal dynamics and competition in determining the isotopic niche breadth of a wetland fish. Freshw. Biol. 58, 780–792. https://doi.org/10.1111/fwb.12084.

Aiken, G.R., Gilmour, C.C., Krabbenhoft, D.P., Orem, W., 2011. Dissolved organic matter in the Florida Everglades: implications for ecosystem restoration. Crit. Rev. Environ. Sci. Technol. 41 (S1), 217–248.

Barron, M., Duvall, S., Barron, K., 2004. Retrospective and current risks of mercury to panthers in the Florida Everglades. Ecotoxicology 13 (3), 223–229.

Belanger, T.V., Scheidt, D.J., Platko II, J.R., 1989. Effects of Nutrient Enrichment on the Florida Everglades. Lake Reservoir Manage. 5, 101–111.

Browder, J.A., Gleason, P.J., Swift, D.R., 1994. Periphyton in the Everglades: Spatial variation, environmental correlates, and ecological implications. Chapter 16. In: Davis, S.M., Ogden, J.C. (Eds.), Everglades: the Ecosystem and its Restoration. St. Lucie Press, Delray Beach, FL.

Davis, S.M., 1994. phosphorus inputs and vegetation sensitivity in the Everglades. In: Davis, S.M., Ogden, J.C. (Eds.), Everglades: The Ecosystem and its Restoration. St. Lucie Press, Delray Beach, Florida, pp. 357–378.

Davis, S.M., J.C. Ogden (Eds.), 1994. Everglades: the Ecosystem and its Restoration. St. Lucie Press, Delray Beach, FL. 826 pp.

Diaz-Ramos, S., D.L. Stevens, Jr., and A.R. Olsen. 1996. EMAP statistical methods manual. U.S. EPA, Corvallis, OR. EPA/620/R-96/002.

Duvall, S., Barron, M., 2000. A screening level probabilistic risk assessment of mercury in Florida Everglades food webs. Ecotoxicol. Environ. Saf. 47, 298–305.

Florida Department of Environmental Protection. 2013. Mercury Total Maximum Daily Load (TMDL) for the State of Florida. October 24, 2013. Florida Department of Environmental Protection, Tallahassee, FL. 120 pp.

Florida Department of Health. 2019. Your guide to eating fish caught in Florida. http://www.floridahealth.gov/programs-and-services/prevention/healthy-weight/nutrition/seafood-consumption/_documents/fish-advisory-big-book2019.pdf.

Friedman, J.H., 2001. Greedy function approximation: a gradient boosting machine. Ann. Stat. 29 (5), 1189–1232.

Gaiser, E.E., 2009. Periphyton as an indicator of restoration in the Florida Everglades. Ecol. Indic. 9 (6S), S37–S45.

Gaiser, E.E., Trexler, J.C., Richards, J.H., Childers, D.L., Lee, D., Edwards, A.L., Scinto, L.J., Jayachandran, K., Noe, G.B., Jones, R.D., 2005. Cascading ecological effects of low-level phosphorus enrichment in the Florida Everglades. J. Environ. Qual. 34, 1–7.

García-Laencina, P., Sancho-Gómez, J., Figueiras-Vidal, A., 2010. Neural Comput. Applic. 19, 263–282. https://doi.org/10.1007/s00521-009-0295-6.

Gilmour, C.C., Henry, A.E., Mitchell, R., 1992. Sulfate stimulation of mercury methylation in freshwater sediments. Environ. Sci. Technol. 26 (11), 2281–2287.

Gilmour C., D. Krabbenhoft, W. Orem, G. Aiken, and E. Roden. 2007. Status report on ACME studies on the Control of Hg methylation and bioaccumulation in the Everglades. 2007 South Florida Environmental Report, Appendix 3B-2, South Florida Water Management District, West Palm Beach, FL, 37 pp.

Greenwell, B., Boehmke, B., Cunningham, J., 2019. gbm: Generalized Boosted Regression Models. R Package Version 2.1.5. https://CRAN.R-project.org/package=gbm.

Gu, B., Chimney, M.J., Newman, J., Nungesser, M.K., 2006. Limnological characteristics of a subtropical constructed wetland in south Florida (USA). Ecol. Eng. 27, 345–360.

Hammerschmidt, C.R., Fitzgerald, W.F., 2006. Bioaccumulation and trophic transfer of methylmercury in Long Island Sound. Arch. Environ. Contam. Toxicol. 51, 416–424. https://doi.org/10.1007/s00244-005-0265-7.

Hart, E.A., Lovvorn, J.R., 2003. Algal vs. macrophyte inputs to food webs of inland saline wetlands. Ecology 84 (12), 3317–3326.

Julian, P., 2016. Appendix 3A-6: water year 2011–2015 annual total phosphorus criteria compliance assessment. 2016 South Florida Environmental Report. Florida Department of Environmental Protection.

Kalla, P.I., D.J. Scheidt. 2017. Everglades ecosystem assessment – Phase IV, 2014: Data reduction and initial synthesis. U.S. EPA, Science and Ecosystem Support Division, Athens, GA. SESD 14-0380. 58 pp. https://www.epa.gov/everglades/everglades-ecosystem-assessment-phase-iv-2014-report.

Kalla, P., M. Cyterski, J. Minucci, D. Scheidt. 2019. Modeling of mercury bioaccumulation in mosquitofish (Gambusia sp.) for the Everglades Regional Environmental Monitoring and Assessment Program. U.S. EPA, Region 4, Laboratory Services and Applied Science Division, Athens, GA. LSASD 20-0085. 35 pp.

Kendall, C., B.E. Bemis, J. Trexler, T. Lange, Q.J. Stober. 2003. Is food web structure a main control on mercury concentrations in fish in the Everglades? Greater Everglades Ecosystem Restoration (GEER) Meeting, Palm Harbor, FL, April 2003. Program and Abstracts.

King, R.S., Richardson, C.J., 2007. Subsidy-stress response of macroinvertebrate community biomass to a phosphorus gradient in an oligotrophic wetland ecosystem. J. N. Am. Benthol. Soc. 26 (3), 491–508. https://doi.org/10.1899/06-002R.1.

Li, Y.B., Mao, Y.X., Liu, G.L., Tachiev, G., Roelant, D., Feng, X.B., Cai, Y., 2010. Degradation of methylmercury and its effects on mercury distribution and cycling in the Florida Everglades. Environ. Sci. Technol. 44 (17), 6661–6666.

Liston, S.E., Trexler, J.C., 2005. Spatiotemporal patterns in community structure of macroinvertebrates inhabiting calcareous periphyton mats. J. N. Am. Benthol. Soc. 24, 832–844.

Liu, G., Cai, Y., Kalla, P., Scheidt, D., Richards, J., Scinto, L., Gaiser, E., Appleby, C., 2008. Mercury mass budget estimates and cycling seasonality in the Florida Everglades. Environ. Sci. Technol. 42, 1954–1960.

Lodge, T.E. 2019. Overview of the Everglades. Chapter 1 in Pollman, C.D., Rumbold, D.G., Axelrad, D.M. (Eds.), Mercury and the Everglades: A Synthesis and Model for Complex Ecosystem Restoration, vol. I – The Evolution of the Everglades as a Perturbed Ecosystem and the Role of Atmospheric Mercury. Springer Nature Switzerland AG 2019. ISBN 978-3-030-20069-5 ISBN 978-3-030-20070-1 (eBook). doi:https://doi.org/10.1007/978-3-030-20070-1.

Loftus, W.F., Trexler, J.C., Jones, R.D., 1998. Mercury transfer through an Everglades aquatic food web. Final Report to the Florida Department of Environmental Protection.

McCormick, P.V., Laing, J.A., 2003. Effects on increased phosphorus loading on dissolved oxygen in a subtropical wetland, the Florida Everglades. Wetl. Ecol. Manag. 11, 199–216.

McCormick, P.V., O'Dell, M.B., 1996. Quantifying periphyton responses to phosphorus in the Florida Everglades: a synoptic-experimental approach. J. N. Am. Benthol. Soc. 15 (4), 450–468.

McCormick, P.C., Newman, S., Miao, S., Reddy, R., Gawlik, D., Fitz, C., Fontaine, T., Marley, D., 1999. Ecological needs of the Everglades. Chapter 3 in Everglades Consolidated Report. South Florida Water Management District.

McCormick, P.V., Newman, S., Vilchek, L.W., 2009. Landscape responses to wetland eutrophication: loss of slough habitat in the Florida Everglades, USA. Hydrobiologia 621, 105–114.

Newman, S., McCormick, P.V., Backus, J.G., 2003. Phosphatase activity as an early warning indicator of wetland eutrophication: problems and prospects. J. Appl. Phycol. 15, 45–59.

Noe, G.B., Childers, D.L., Jones, R.D., 2001. Phosphorus biogeochemistry and the impact of phosphorus enrichment: why is the Everglades so unique? Ecosystems 4, 603–624.

Olsen, A.R., Sedransk, J., Edwards, D., Gotway, C.A., Liggett, W., 1999. Statistical Issues for monitoring ecological and natural resources in the United States. Environ. Monit. Assess. 54, 1–45.

Olsen, A.R., Kincaid, T.M., Kentula, M.E., Weber, M.H., 2019. Survey design to assess condition of wetlands in the United States. Environ. Monit. Assess. 191 (Suppl. 1), 268. https://doi.org/10.1007/s10661-019-7322-6.

Orem, W., Gilmour, C., Axelrad, D., Krabbenhoft, D., Scheidt, D., Kalla, P., McCormick, P., Gabriel, M., Aiken, G., 2011. Sulfur in the South Florida ecosystem: distribution, sources, biogeochemistry, impacts, and management for restoration. Crit. Rev. Environ. Sci. Technol. 41 (sup1), 249–288. https://doi.org/10.1080/10643389.2010.531201.

Pollman, C.D., 2014. Mercury cycling in aquatic ecosystems and trophic state-related variables – implications from structural equation modeling. Sci. Total Environ. 499, 62–73. https://doi.org/10.1016/j.scitotenv.2014.08.036.

R Core Team, 2018. R: A Language and Environment for Statistical Computing. R Foundation for Statistical Computing, Vienna, Austria https://www.R-project.org/.

Ramsar Convention, 2006. The List of Wetlands of International Importance, Version of 7 December 2006. http://www.ramsar.org/sitelist.pdf. (Accessed 13 December 2006).

Regnell, O., Watras, C.J., 2019. Microbial mercury methylation in aquatic environments: a critical review of published field and laboratory studies. Environ. Sci. Technol. 53 (1), 4–19. https://doi.org/10.1021/acs.est.8b02709.

Rumbold, D.G., 2005. A probabilistic risk assessment of the effects of methylmercury on great egrets and bald eagles foraging at a constructed wetland in south Florida relative to the Everglades. Hum. Ecol. Risk. Assess. 11, 365–388.

Rumbold, D.G. 2019a. The evolution of the Everglades as a perturbed ecosystem. Chapter 2 in Pollman, C.D., Rumbold, D.G., Axelrad, D.M. (Eds.), Mercury and the Everglades: A Synthesis and Model for Complex Ecosystem Restoration, vol. I – The Evolution of the Everglades as a Perturbed Ecosystem and the Role of Atmospheric Mercury. Springer Nature Switzerland AG 2019. ISBN 978-3-030-20070-1 (eBook). doi:https://doi.org/10.1007/978-3-030-20070-1.

Rumbold, D.G. 2019b. Regional-scale ecological risk assessment of mercury in the Everglades and South Florida. Chapter 10 in Pollman, C.D., Rumbold, D.G., Axelrad, D.M. (Eds.), Mercury and the Everglades: A Synthesis and Model for Complex Ecosystem Restoration, vol. II – Aquatic Mercury Cycling and Bioaccumulation in the Everglades. Springer Nature Switzerland AG 2019. ISBN 978-3-030-32057-7 (eBook). doi:https://doi.org/10.1007/978-3-030-32057-7.

Rumbold, D.G., Lange, T.R., Axelrad, D.M., Atkeson, T.D., 2008. Ecological risk of methylmercury in Everglades National Park, Florida, USA. Ecotoxicology 17, 632–641.

Sarker, S.K., Kominoski, J.S., Gaiser, E.E., Scinto, L.J., Rudnick, D.T., 2020. Quantifying effects of increased hydroperiod on wetland nutrient concentrations during early phases of freshwater restoration of the Florida Everglades. Restor. Ecol. https://doi.org/10.1111/rec.13231.

Scheidt, D.J., P.I. Kalla. 2007. Everglades Ecosystem Assessment: Water Management and Quality, Eutrophication, Mercury Contamination, Soils and Habitat: Monitoring for Adaptive Management: A R-EMAP Status Report. USEPA Region 4, Athens, GA. EPA 904-R-07-001. 98 pp. https://www.epa.gov/everglades/everglades-ecosystem-assessment-water-management-and-quality-eutrophication-mercury.

Scheidt, D., J. Stober, R. Jones, K. Thornton. 2000. South Florida ecosystem assessment: water management, soil loss, eutrophication and habitat. United States Environmental Protection Agency Report 904-R-00-003. 46 pp. http://www.epa.gov/region4/sesd/reports/epa904r00003.html.

Seixas, T.G., Moreira, I., Siciliano, S., Malm, O., Kehrig, H.A., 2014. Differences in methylmercury and inorganic mercury biomagnification in a tropical marine food web. Bull. Environ. Contam. Toxicol. 92, 274–278. https://doi.org/10.1007/s00128-014-1208-7.

Sellers, P., Kelly, C.A., Rudd, J.W.M., MacHutchon, A.R., 1996. Photodegradation of methylmercury in lakes. Nature 380, 694–697.

Sellers, P., Kelly, C.A., Rudd, J.W.M., 2001. Fluxes of methylmercury to the water column of a drainage lake: the relative importance of internal and external sources. Limnol. Oceanogr. 46 (3), 623–631.

South Florida Water Management District. 2016. South Florida environmental report: Appendix 3-1: annual permit report for the Everglades Stormwater Treatment Areas, permit report (May 1, 2014 - April 30, 2015, permit 0311207).

Spalding, M.G., Frederick, P.C., McGill, H.C., Bouton, S.N., McDowell, L.R., 2000. Methylmercury accumulation in tissues and its effects on growth and appetite in captive great egrets. J. Wildl. Dis. 36 (3), 411–422.

Stevens Jr., Don L., 1997. Variable density grid-based sampling designs for continuous spatial populations. Environmetrics 8, 167–195.

Stevens Jr., D.L., Olsen, A.R., 2004. Spatially-balanced sampling of natural resources. J. Am. Stat. Assoc. 99 (465), 262–278. https://doi.org/10.1198/016214504000000250.

Stober, Q.J., K. Thornton, R. Jones, J. Richards, C. Ivey, R. Welch, M Madden, J. Trexler, E. Gaiser, D. Scheidt, S. Rathbun. 2001. South Florida ecosystem assessment: Phase I/II – Everglades stressor interactions: hydropatterns, eutrophication, habitat alteration, and mercury contamination. EPA 904-R-01-002.

Tai, C., Li, Y., Yin, Y., Scinto, L.J., Jiang, G., Cai, Y., 2014. Methylmercury photodegradation in surface water of the Florida Everglades: importance of dissolved organic matter-methylmercury complexation. Environ. Sci. Technol. 48, 7333–7340. https://doi.org/10.1021/es500316d.

Thornton, K.W., G.E. Saul, D.E. Hyatt. 1994. Environmental monitoring and assessment program assessment framework. United States Environmental Agency Report EPA/620/R-94/016. Research Triangle Park, North Carolina. 47 pp.

U.S. Army Corps of Engineers and South Florida Water Management District, 2014. Central Everglades Planning Project. https://www.saj.usace.army.mil/Portals/44/docs/Environmental/CEPP/01_CEPP%20Final%20PIR-EIS%20Main%20Report.pdf. (Accessed 24 June 2020).

USEPA. 1995. Environmental Monitoring and Assessment Program (EMAP) Cumulative Bibliography. United States Environmental Protection Agency, Office of Research and Development. EPA/620/R-95/006. Research Triangle Park, North Carolina. 44 p.

USEPA, 2021. Environmental monitoring in the Everglades. Everglades REMAP Web Page. 1993–2014 https://www.epa.gov/everglades/environmental-monitoring-everglades.

Vijayaraghavan, K., C.D. Pollman. 2019. Mercury emission sources and contributions of atmospheric deposition to the Everglades. Chapter 5 in C.D. Pollman, D.G. Rumbold, D.M. Axelrad (Eds.), Mercury and the Everglades: A Synthesis and Model for Complex Ecosystem Restoration, vol. I – The Evolution of the Everglades as a Perturbed Ecosystem and the Role of Atmospheric Mercury. Springer Nature Switzerland AG 2019. ISBN 978-3-030-20070-1 (eBook). doi:10.1007/978-3-030-20070-1doi:10.1007/978-3-030-20070-1_5.

Walters, D.M., Cross, W.F., Kennedy, T.A., Baxter, C.V., Hall Jr., R.O., Rosi, E.J., 2020. Food web controls on mercury fluxes and fate in the Colorado River, Grand Canyon. Sci. Adv. 6, eaaz4880.

Wang, Y., Gu, B., Lee, M.K., Jiang, S.J., Xu, Y.F., 2014. Isotopic evidence for anthropogenic impacts on aquatic food web dynamics and mercury cycling in a subtropical wetland ecosystem in the US. Sci. Total Environ. 487, 557–564.

Williams, A.J., Trexler, J.C., 2006. A preliminary analysis of the correlation of food-web characteristics with hydrology and nutrient gradients in the southern Everglades. Hydrobiologia 569, 493–504.

Zabala, J., Trexler, J.C., Jayasena, N., Frederick, P., 2020. Early breeding failure in birds due to environmental toxins: a potentially powerful but hidden effect of contamination. Environ. Sci. Technol. 54 (21), 13786–13796. https://doi.org/10.1021/acs.est.0c04098.

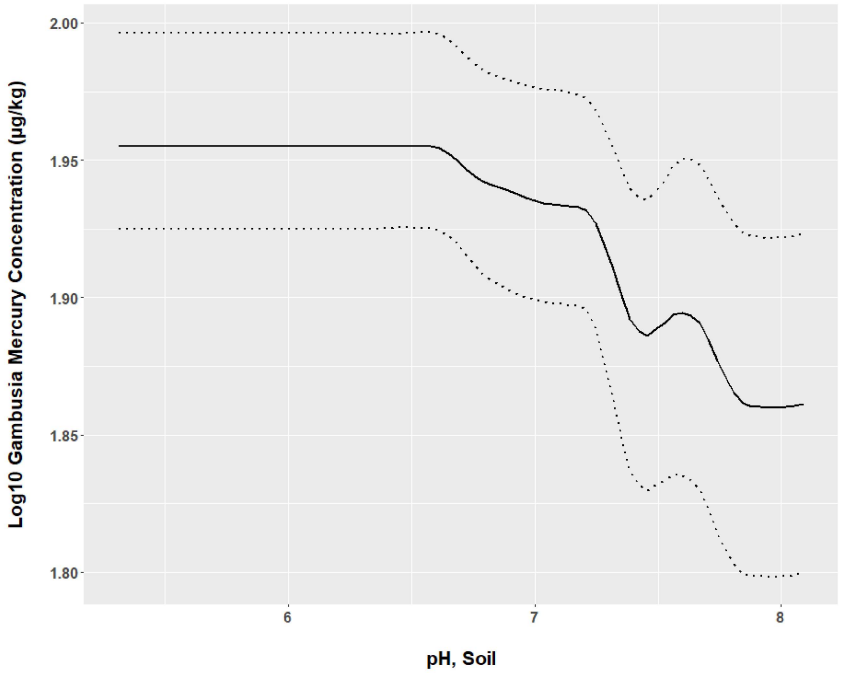

Figure S1a. PDP of mosquitofish Log_{10} mercury (µg kg^{-1}) on soil pH (S.U.). The dashed lines represent the 2.5th and 97.5th percentiles of the variability seen in 200 GBM model runs.

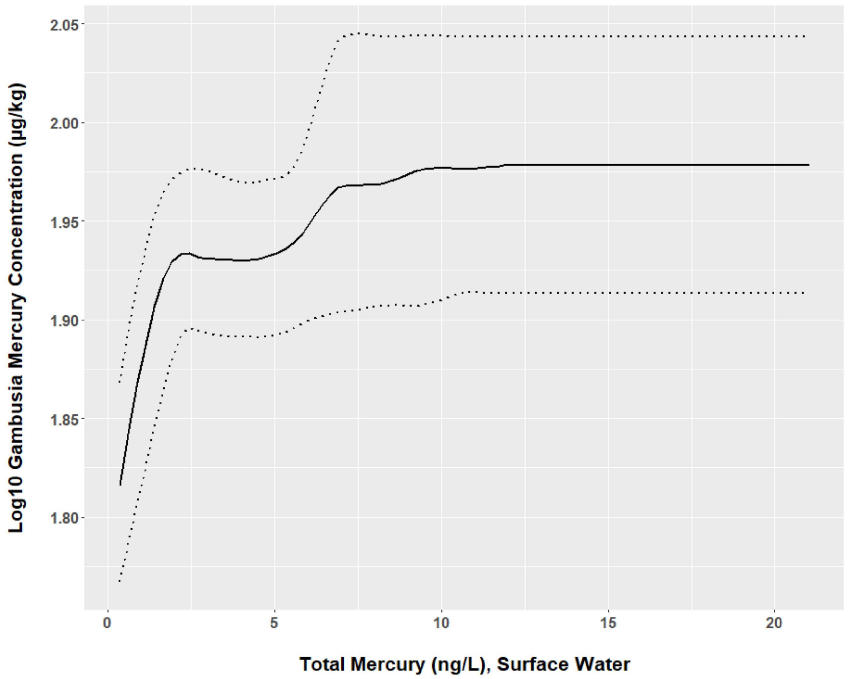

Figure S1b. PDP of mosquitofish Log_{10} mercury (µg kg^{-1}) on total mercury (ng L^{-1}) in surface water. The dashed lines represent the 2.5th and 97.5th percentiles of the variability seen in 200 GBM model runs.

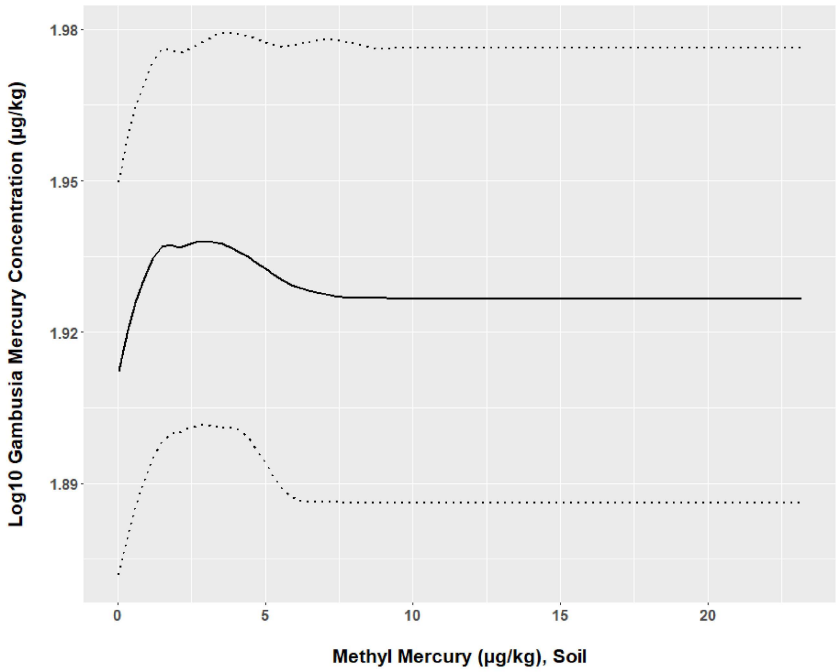

Figure S1c. PDP of mosquitofish Log_{10} mercury (µg kg^{-1}) on methyl mercury in soil (µg/kg). The dashed lines represent the 2.5th and 97.5th percentiles of the variability seen in 200 GBM model runs.

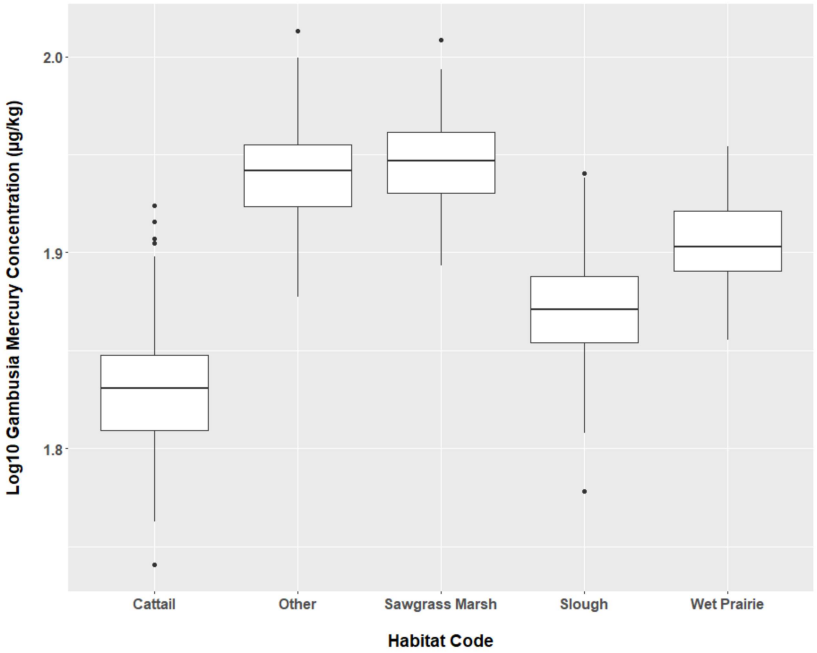

Figure S1d. PDP of mosquitofish Log_{10} mercury (µg kg^{-1}) on habitat code. The boxes are the interquartile range and the hozontal lines are the median.

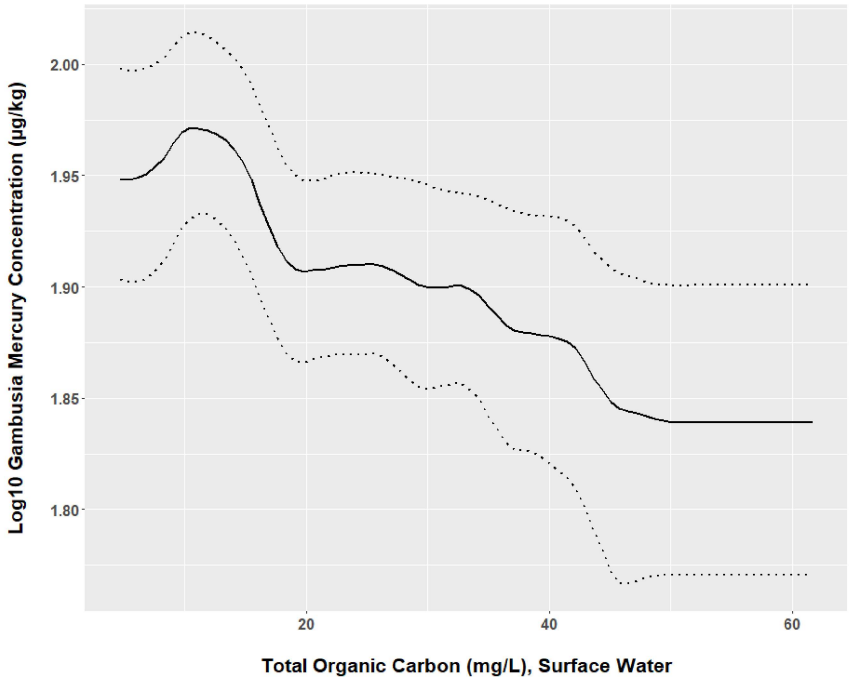

Figure S1e. PDP of mosquitofish Log_{10} mercury (µg kg^{-1}) on total organic carbon (mg L^{-1}) in surface water. The dashed lines represent the 2.5th and 97.5th percentiles of the variability seen in 200 GBM model runs.

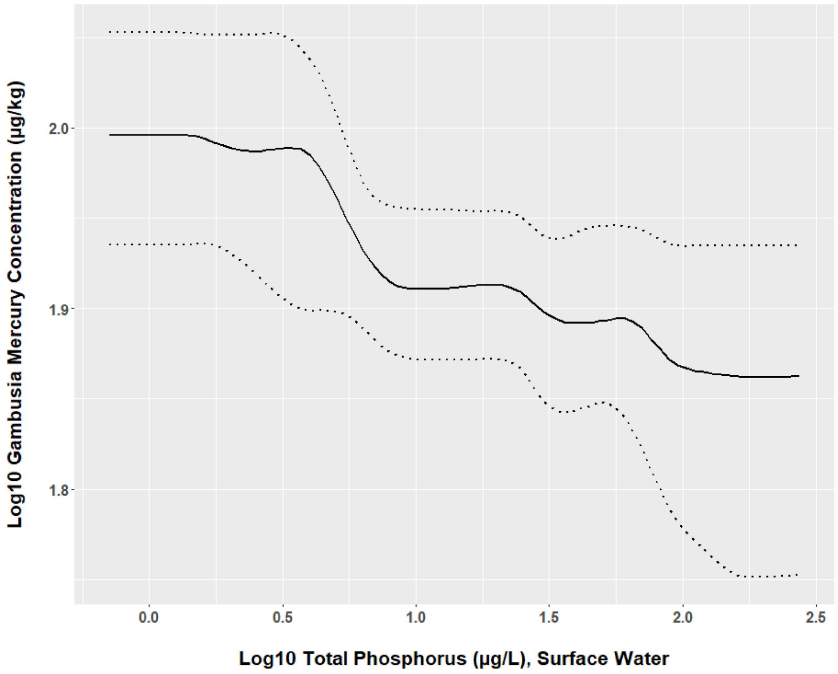

Figure S1f. PDP of mosquitofish Log_{10} mercury (µg/kg) on Log_{10} total phosphorus in surface water (µg/L). The dashed lines represent the 2.5th and 97.5th percentiles of the variability seen in 200 GBM model runs.

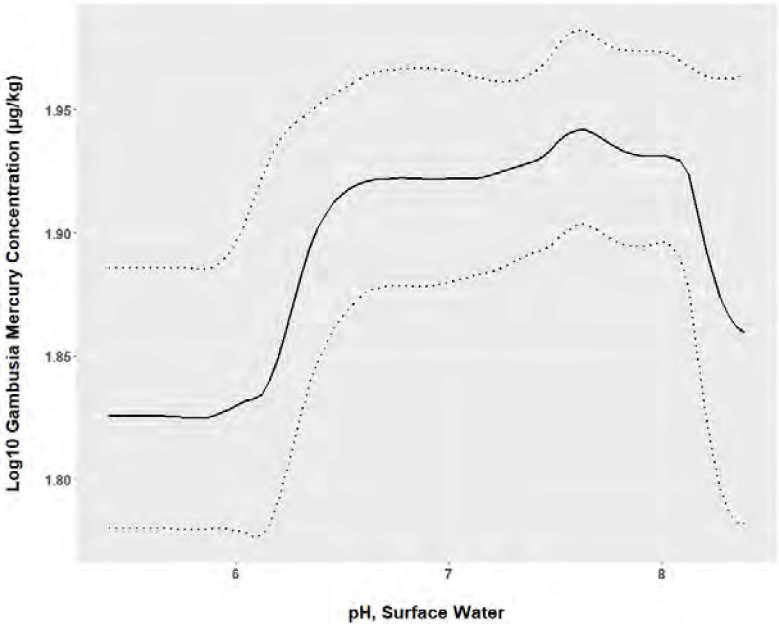

Figure S1g. PDP of mosquitofish Log_{10} mercury (µg/kg) on pH of surface water (S.U.). The dashed lines represent the 2.5th and 97.5th percentiles of the variability seen in 200 GBM model runs.

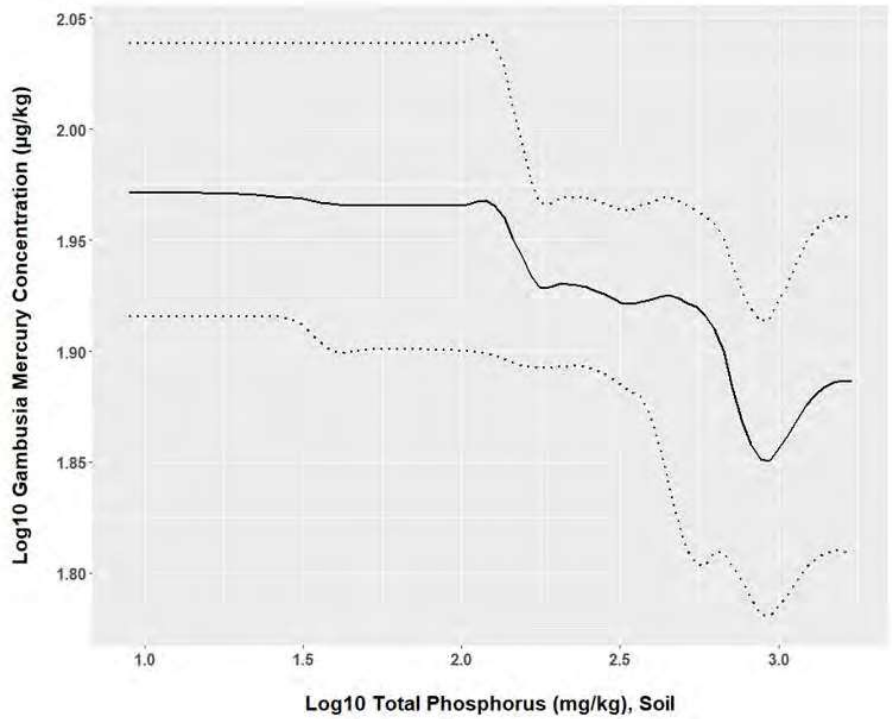

Figure S1h. PDP of mosquitofish Log_{10} mercury (µg/kg) on Log_{10} total phosphorus in soil (mg/kg). The dashed lines represent the 2.5th and 97.5th percentiles of the variability seen in 200 GBM model runs.

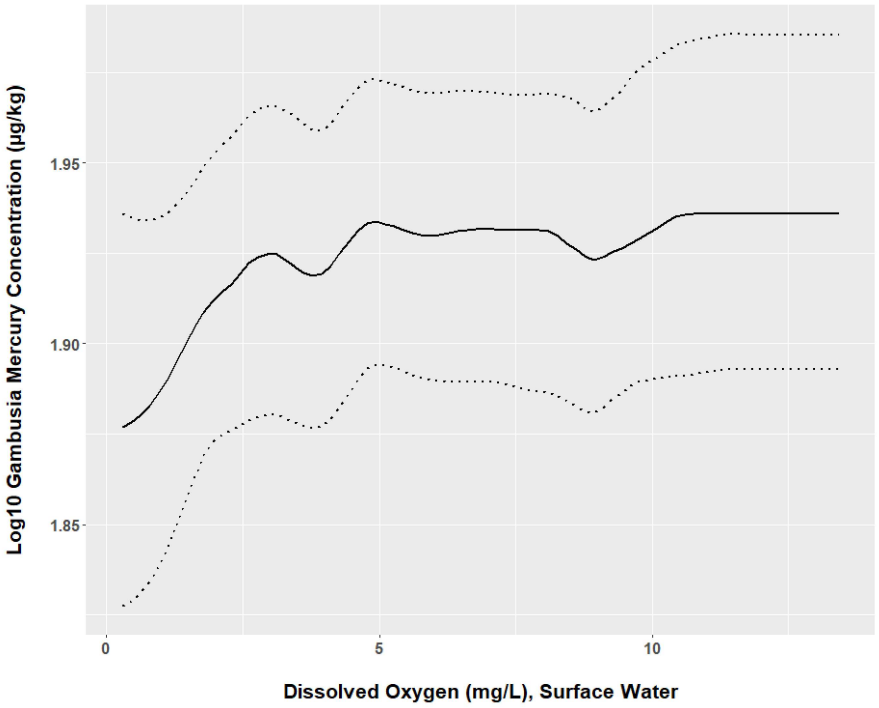

Figure S1i. PDP of mosquitofish Log_{10} mercury (µg/kg) on dissolved oxygen in surface water (mg/L). The dashed lines represent the 2.5^{th} and 97.5^{th} percentiles of the variability seen in 200 GBM model runs.